RSC Advances

ROYAL SOCIETY
OF **CHEMISTRY**

www.rsc.org/advances

Journal Name

ARTICLE

Full Factorial Design applied to the synthesis of PdAg nanobars by the polyol method and the perspective for ethanol oxidation

R. Carrera-Cerritos,[a] C. Ponce de León,[b] J. Ledesma-García,[c] R. Fuentes-Ramírez[a] and L. G. Arriaga*[d]

Abstract. Full Factorial design methodology was applied for the first time to the synthesis and optimization of palladium/silver nanobars using the polyol process as reducer. The concentration of Br$^-$ ions, the temperature and time of the reaction were selected as factors to study, whereas the yield (% nanobars) was the response to be analyzed. The nanoparticles were characterized by XRD, EDX, TEM, HRTEM, XPS, and tested for the ethanol electro-oxidation reaction by cyclic voltammetry in alkaline solution. The three factors had a positive effect on the response, the nanobar yield increases as the level of the variables changed from -1 to +1. The temperature and reaction time are the most determinant variables (main and interacting) on the nanobar yield, while the Br$^-$ concentration influenced to a less extent. After designing three optimal experiments, a maximum nanobar yield of 47.3 % was obtained. The more negative electro-oxidation onset, higher current density and more negative current peak potential showed that the incorporation of Ag in Pd nanobar improves the kinetic and thermodynamic behavior towards the ethanol electro-oxidation reaction in comparison to that obtained on nanometric pure Pd nanobars. This improvement is the result of the surface modification caused by the Ag incorporation in the formation of the PdAg bimetallic nanobars with (2 0 0) surfaces.

1 Introduction

The synthesis of metallic nanobars has attracted great attention in recent years in electro catalysis, due to their enhanced catalytic specific activity for the electro-oxidation of methanol, formic acid and dimethyl ether. Metallic nanoparticles owe their catalytic activity to the preferential exposure of their crystalline faces .[1]

[a]Departamento de Ingeniería Química, Universidad de Guanajuato, División de Ciencias Naturales y Exactas, Guanajuato, Gto., C.P. 36050, México. Tel.: +52 4737320006-1426; E-mail:rosalba@ugto.mx.

[b]Electrochemical Engineering Laboratory, Energy Technology Research Group, University of Southampton, Highfield, Southampton, Hampshire SO17 1BJ, UK.Fax:+44 0 2380597051; Tel:+44 02380598931; E-mail:c.a.ponce-de-leon-albarran@soton.ac.uk.

[c]Facultad de Ingeniería, División de Investigación y Posgrado, Universidad Autónoma de Querétaro, Querétaro, Qro., C.P. 76010, México. E-mail: janet.ledesma@uaq.mx

[d]Centro de Investigación y Desarrollo Tecnológico en Electroquímica, Parque Tecnológico Querétaro s/n, Sanfandila, Pedro Escobedo, Qro., C.P. 76703, México. Fax: +52 4422116001, Tel: +52 4422116001; E-mail: larriaga@cideteq.mx.

In the case of Pd, it has been reported that Pd nanobars in acidic and alkaline media offer superior electrocatalytic activity for the oxygen reduction reaction (ORR), compared with those of spherical shape and Pd bulk.[2]

The specific activity of Pd nanobars of 48 nm height was almost three times greater than 9 nm diameter Pd nanoparticles in H_2SO_4–methanol electrolyte, thus showing nanobar's high tolerance properties against the poisoning effect of methanol.[3] From theoretical Density Functional Theory (DFT) calculations and from experimental results, a similar enhanced behavior of Pd nanobars has been observed in the electrocatalytic activity of the ethanol reaction in alkaline medium. This enhanced performance was attributed to the prevalence of Pd (1 0 0) faces.[4]

Palladium-based alloys have been selected as catalysts in many important physical processes, chemical and electrochemical reactions including: hydrogen separation from gaseous mixtures without further purification using membrane technologies,[5] oxygen reduction reaction,[6] and direct oxidation of alcohols; such as methanol, ethanol, formic acid, and ethylene glycol.[7] Among the number of palladium-based alloys, PdAg nanoparticles have received increased attention due to their higher catalytic and electrocatalytic properties compared with those of monometallic Pd nanoparticles.[8] Moreover, the synergetic interaction between Pd and Ag atoms not only produces materials that exhibit excellent catalytic activity, but also enhances the tolerance of adsorbed CO and improves the stability for ethanol electro oxidation in comparison to

Pd/C catalyst.[9]Considering this background, interesting electro catalytic properties could be inferred by the morphologic manipulation of PdAg alloyed nanoparticles when compared with typical spherical PdAg nanoparticles or monometallic Pd nanoparticles. To the authors' knowledge, the synthesis of 10 nm PdAg nanobars has not been reported in the literature and therefore the objective of this paper is to analyze their synthesis using the polyol method.

Among the number of chemical methods existing, polyol process is the technology most commonly used for the synthesis of Pd nanobars due to its relative simplicity and easy scale up potential.[4b,10] Previous reports have shown that the formation of Pd nanobars using the polyol synthesis method can be influenced by temperature, concentration of Br- ions, and reactiontime.[4b,10] The novelty of this paper is based on the fact that this method has not been extended to prepare bimetallic or multi-metallic nanobars.

Factorial design is an experiment design methodology that enables:a) among thevariables studied, the determination of themain factor that impact the response by analyzing the effects plots, b) the study of the parallel effects of two or more factors on the responses studied and c) faster optimization of the response by manipulating the main factor that impacted the response.[11] This information can be obtained with a relative small number of runs per factor, thus making the experimentation process quicker and cheaper than the traditional approach of "one factor at a time" method, in which experimental factors are varied one at a time while the remaining factors are held constant. For these reasons, this methodology has recently been successfully applied to the synthesis of nanoparticles, including lanthanum oxide and silver nanoparticles.[11,12] In the present study, a full factorial design 2^3 was designed and applied to the synthesis and optimization of PdAg nanobars by the polyol method. The concentration of Br- ions, the temperature and time of the reaction were selected as the main factors to study, whereas the nanobar yield (% nanobars) was the response studied. The PdAg bimetallic nanoparticles were characterized by Electron Microscopy Transmission (TEM), X-Ray Diffraction (XRD) and High Resolution Transmission Electron Microscopy (HRTEM), X-Ray Photoelectron Spectroscopy (XPS), and tested for the ethanol electro-oxidation reaction by cyclic voltammetry in alkaline solution.

2 Experimental

2.1 Experiment design

An experimental design with two levels and three variables (2^3) full factorial planning was performed to synthesize PdAg nanobars by the polyol process. The selection of experimental factors is a crucial step in the factorial experimental designs. Careful selection of the key factors determines the success of the factorial design. In this work, we have selected three factors to be analyzed (Table 1). The selection was performed considering our previous experience producing pure Pd nanobars, and reported polyol methodologies.[4b,10a] In the 2^3 full factorial design, it is postulated that the final properties obtained by experiments can be expressed as a linear function of experimental factors. Therefore, the experiments were designed at only two levels for each factor. As this paper reports the first inspection to the factorial design applied to the synthesis of PdAg nanobars, the curvature was no verified by performing experiments at the center point. The experimental domain of each factor (X) is expressed with the maximum and minimum values taken during the experimentation. Then a coded notation -1 for the lowest level and +1 for the highest level (- and + to simplify) was assigned.

Table 1 Chosen factors and experimental domain.

Factors	Experimental domain	
	Level (-)	Level (+)
X_1= Temperature (K)	373	400
X_2= Time (h)	1	3
X_3= Br- concentration (g)	0.6	1.2

The experimental design and polynomial models were fitted using the MiniTab 16 Statistical Software. The mathematical model of Equation 1 was applied to describe the principal factors and interactions among the studied variables:[13]

$$Y(\%) = \beta_0 + \beta_1 X_1 + \beta_2 X_2 + \beta_3 X_3 + \beta_{12} X_1 X_2 + \beta_{13} X_1 X_3 + \beta_{23} X_1 X_2 + \varepsilon$$
(1)

Coded (-1,+1) levels were used for each independent variable X_1, X_2 and X_3, in which the -1 level corresponds to the lower value of each variable and +1 to the higher one. The choice of these values was based on acceptable domains for each variable, considering previous reports for nanobar synthesis. After analyzing the effect plots, three experiments were designed and performed around these domains in order to optimize the response.

2.2 Synthesis example

The PdAg nanobars were synthesized using a modified method for obtaining pure Pd nanobars.[4b,10a] In the case of Exp. 1 (Table 2), 5 cm^3 of ethylene glycol (EG, J.T. Baker, Austin, TX, USA, 99.9%) were placed in a 25 cm^3 three-neck flask equipped with a reflux condenser and a PTFE-coated magnetic stirring bar. The flask was heated with an oil bath and stirred under static air at constant temperature of 373 K. Meanwhile, 0.024 g of Na$_2$PdCl$_4$ (Sigma-Aldrich, St. Louis, MO, USA, 98%) and 0.6 g of KBr (J.T. Baker, Austin, TX, USA, 99%) were dissolved in 3 cm^3 of deionized water; and 0.0916 g of polyvinylpyrrolidone (PVP, Aldrich, St. Louis, MO, USA, Mw = 55,000) and 0.019 g of AgNO$_3$ (J.T. Baker, Austin, TX, USA, 99%) were dissolved in 3 cm^3 of EG at room temperature (298 K). The two solutions were then injected simultaneously into the three-neck flask using two syringe pumps (Cole Palmer Instruments Company, Vernon Hills, IL, USA) at a rate of 45 cm^3 h^{-1}. The reactive mixture was heated at 373 K. After 1 h, the reaction was cooled down to room temperature and the product was separated by adding 30 cm^3 of ketone and centrifuged at 4000 rpm for 20 min. The AgPd nanoparticles were redispersed in deionized water and separated by ultracentrifugation at 35000 rpm for 2 h. The last process was repeated several times to remove the remaining impurities. Finally, the product was dried at 333 K for 12 h.

2.3 Materials characterization

The crystallinity nature of the PdAg nanoparticles was investigated using a Bruker D8 Advance, X-ray diffractometer, operated using Cu-Kα radiation at 40 kV and 40 mA over a 2θ range of 30–90 with a step size of 0.05°, and a step time of 1 s. The diffraction patterns were compared to the Joint Committee on Powder Diffraction Standards (JCPDS); crystalline size composition was calculated from XRD patterns employing the Rietveld analysis and using the TOPAS software. A JEOL JEM-100Sand JEOL JEM-1010 operating at 60 kV and 100 kV, respectively were utilizedfor Transmission Electron Microscopy (TEM) and EDX analyses. The specimens were

prepared by ultrasonic dispersion in isopropyl alcohol and depositing a drop of suspension on acarbon-coated grid before TEM session. HRTEM analyses were conducted on a Titan 80-300 FEI apparatus operated at 300 kV to observe the detailed morphology and further to calculate of Fast Fourier Transform (FFT) to obtain the diffraction electron pattern. The XPS characterizations were carried out with a Versaprobe PHI 5000 system using Al monochromatic X-ray at 25 W and 15 kV. The survey and detailed spectra were obtained from 1-1000 eV and 331-345 eV, step size of 0.5 eV and 0.05 eV, and pass energy of 117.4 and 23.5 eV, respectively. The C 1s peak was used as standard for shifting corrections.

2.4 Electrochemical experiments

All electrochemical measurements were conducted in a three-electrode cell at room temperature connected to a potentiostat/galvanostat Autolab PSSTAT 302. An Hg/HgO in 1 M KOH and a platinum foil electrode were used as the reference electrode and counter electrode, respectively. The working electrode was prepared using a glassy carbon (GC) disc measuring 3 mm in diameter, which was previously polished with alumina powder (0.05 μm), sonicated for 10 min and washed with deionized water. During the electrochemical measurements, a mixture containing 1.0 mg of electrocatalyst and 73 μL of isopropyl alcohol (Baker, 99.9%) was pretreated for 20 min under ultrasonication. Then, 7 μL of Nafion® solution (5% isopropyl alcohol, Electrochem) was added to the mixture and sonicated for 20 min again to obtain a well-dispersed ink. A 2.2 μL portion of the catalyst ink was then transferred onto the surface of the GC electrode and dried in air to obtain a catalyst thin film. Cyclic voltammetry (CV) was performed in aqueous solutions of 1 M KOH in both the absence and presence of ethanol solutions of various concentrations from −1 to 0.4 V (vs. NHE) at 0.05 V s^{-1}. The electrochemical cycling done in 1M KOH solution (without ethanol) was used as an additional cleaning treatment of the material. On the other hand, the reported electro-oxidation cycle was the tenth, where the electrochemical signal has been stabilized.

3 Results and Discussion

3.1 Morphology and size

Figure 1 shows the TEM images for the PdAg nanoparticles that resulted from each run.

Fig. 1 (Exp. 1) corresponds to the product obtained by using the same conditions used by other authors to synthesize pure Pd nanobars.[4b,10a] However, the small nanobar yield was evident as the image shows a mixture of irregular PdAg nanoparticles of ~ 5 to 20 nm diameter. This result suggested that big changes in the methodology had to be made to improve nanobar formation. As shown in Fig. 1 (Exp. 2), most of the nanoparticles consisted of irregular forms with an average size of ~7 nm. However, a few PdAg nanobars with an average particle size of approximately 5-7 nm (width) × 7-9 nm (length) could beobserved. X-ray energy dispersed counts indicated that bigger nanoparticles (Exp 2) were composed by 88 % Ag and 12 % Pd, whereas the smaller ones contained 92 % Pd and 8 % Ag (Spectrum not shown). Figures for Exp. 3, 5 and 7 show a mixture of small nanoparticles and big agglomerates; among the small nanoparticles, irregular and rectangular nanoparticles (the amount and size of the nanoparticles are detailed and discussed in further sections) can be observed. On the other

hand, the number of PdAg nanobars was notably higher in Fig. 1 (Exp. 4 and 8). Moreover, the composition of the small nanoparticles was found to be 88.5% Pd and 11.5 % Ag. This result showed for the first time, the formation of bimetallic PdAg nanobars smaller than 10 nm by polyol method.
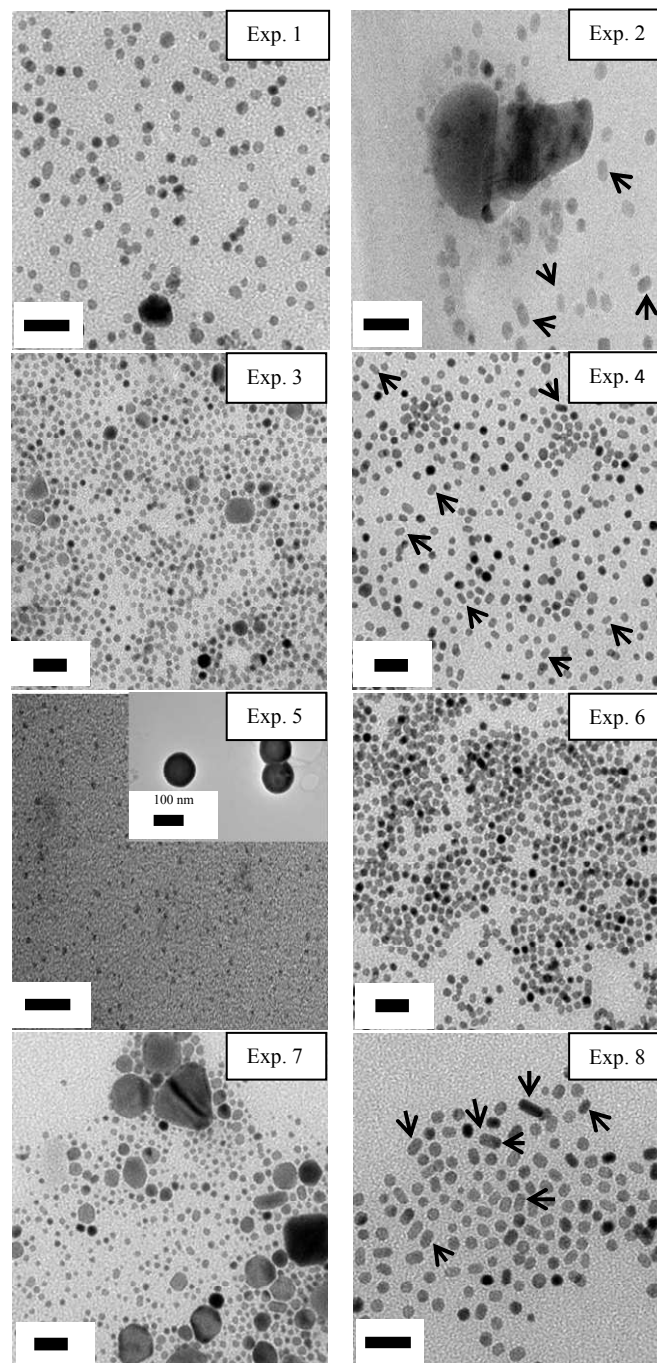

Fig.1 TEM images of all the experiments resulted of combining the factors and levels. The exact value of the experimental conditions is shown in Table 2. The amount of PVP, H$_2$O, ethylenglycol were maintained constants in all the experiments. A few arrows were set to indicate nanobars in the image. Scale bar: 20 nm.

3.2 Model fitting

Table 2 shows all the runs (2^3) or experiments resulting from the factor level combination, according to the full factorial

experiments design methodology.[13] The factor levels are expressed in the Matrix of experiments with coded units such as - and +, whereas the numerical values of such codes are detailed in the experimentation plan. The sequence of runs was performed randomly in order to eliminate any influence of systematic errors which are difficult to stabilize and control. The response (% nanobars) is shown in the last column (Table 2).

Table 2 Matrix of experiments for a 2^3 completed factorial design, experimentation plan and measured responses.

	Matrix of experiments			Experimentation plan			Response
Exp.	X_1	X_2	X_3	**T (K)**	**Time (h)**	**KBr (g)**	**(%)**
1	-	-	-	373	1	0.6	1.3
2	+	-	-	400	1	0.6	8.9
3	-	+	-	373	3	0.6	3.1
4	+	+	-	400	3	0.6	23.7
5	-	-	+	373	1	1.2	0
6	+	-	+	400	1	1.2	2.5
7	-	+	+	373	3	1.2	3
8	+	+	+	400	3	1.2	43

The effects of the independent variables on the size of PdAg nanobars were investigated using the lineal model, which was estimated based on the experimental results with the respective coefficients as given in Eq. (2).

$$Y(\%) = 10.65 + 8.79X_1 + 7.46X_2 + 1.46X_3 + 6.27X_1X_2 + 1.82X_1X_3 + 3.40X_2X_3 \qquad (2)$$

Where, $Y(\%)$ is the PdAg-nanobar yield calculated by counting the amount of PdAg nanobars found in the TEM images (considering 100 nanoparticles, at least). The analysis of variance based on ANOVA test for this regression model is listed in Table 3. The model equation for the PdAg nanobar preparation falls in the limit of a well-described model within the range of the independent variables. The F-value of 3.29 indicates that the model is not significant for PdAg nanobar synthesis because a value greater than 4 is considered desirable.[14] The p-value of the model is considered to be significant when it falls below 0.05 while values greater than this value are considered as not significant. The results of the model indicated that it is non-significant according to the p-values slightly greater than 0.05, as shown in Table 3. The correlation coefficients of R^2 and R^2_{adj} for this model were found to be 0.95 and 0.6627, respectively, indicating a good fit between the regression model (Equation 2) and the experimental values (Table 2).

Source	C	DOF	(SS)	SS Adjust	MS	F	T	P
C	10.65						3.44	0.18
X_1	8.79	1	619.34	619.34	619.34	8.06	2.83	0.216
X_2	7.46	1	445.96	445.96	445.95	5.80	2.40	0.25
X_3	1.46	1	17.2	17.2	17.19	0.22	0.47	0.72
X_1*X_2	6.27	1	315.13	315.13	315.13	4.10	2.02	0.29
X_1*X_3	1.82	1	26.68	26.68	26.68	0.34	0.58	0.66
X_2*X_3	3.40	1	92.96	92.96	92.95	1.21	1.1	0.47
Reg.		6	1517.27	1517.27	252.87	3.29		0.39
Error		1	76.82	76.82	76.81			
Total		7	1594.09					

* S= 8.76459, R^2= 95.18 %, Significance value = 5%, C: Coefficient, DOF: Degrees of Freedom, SS: Sum of Squares, MS: Mean Square.

Table 3 ANOVA parameters obtained for the fitting of Eq. 2.

Even though the F and p-value of the model are in the limit of acceptance, it should be noted that the formation of small PdAg nanobars with less than 10 nm was observed for the first time by using the polyol process. Moreover, the T-values for the temperature, reaction time and temperature-reaction time interactioncoefficients are greater than the KBr containing parameters, thus showing the high significance of these factors on the PdAg nanobar yield. These results suggest that the analysis of these factors and interactions can conduce to improved response, as it is shown in further sections.
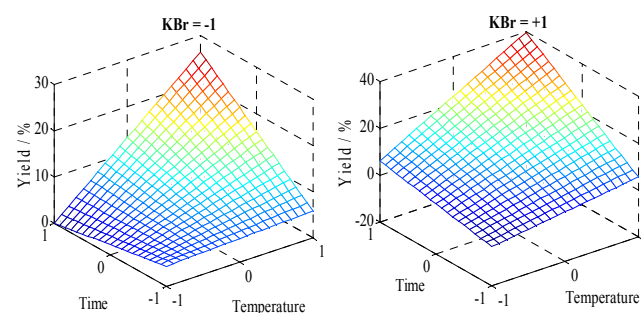

Fig. 2 Plots of the PdAg nanobar yield calculated using the model obtained (Eq.2).

3.3 Analysis of main factors and interactions

The plots of the main effects on the formation of the nanobars is shown in Figure 3in order to analyse the influence of each variable on the nanobar yield. The results showed that the three factors have a positive effect on the response;the nanobar yield increases as the level changed from -1 to +1. This result is also evident in Table 3, considering that a positive coefficient sign indicates an increase in nanobar yield. Additionally, in the considered range of parameters, the temperature and reaction time presented high slopes resulting from their strongest effect on the nanobar yield; whereas the Br$^-$ concentration impacted in less extent the nanobar formation. The following sections describe in detail these main effects.
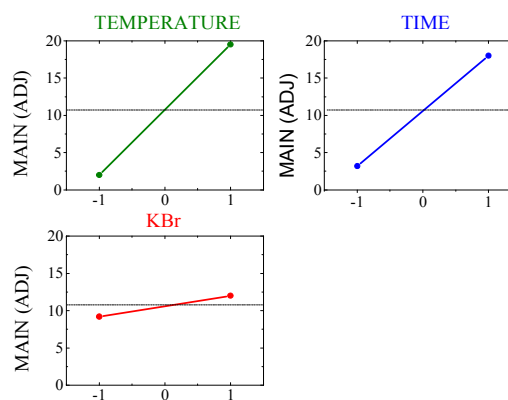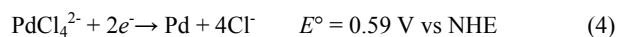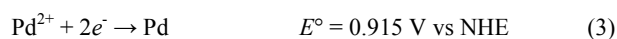

Fig. 3 Plot of the main effects for the full factorial design.

3.3.1 Effect of Br- concentration. It has been demonstrated that bromide can chemisorb onto the surface of palladium seeds and alter the order of surface free energies for different facets so the formation of (100) surface can be strongly

promoted to generate nanocubes and nanobars.[15]In the present study, bromide also played an important role in promoting the (100) facets resultingin the formation of square shaped nanostructures. However, it is believed that the addition of bromide also contributed to the slow reduction because the overall stability constant of $PdBr_4^{2-}$ is nearly 10^4 times higher than that of $PdCl_4^{2-}$, almost all chloride in the $PdCl_4^{2-}$ ions can be substituted by bromide to form complex ions $PdBr_4^{2-}$ when the $Na_2PdCl_4$is mixed with KBr in water.[10a]According to thermodynamic calculations, the potential of palladium precursor (Na_2PdCl_4) is greatly reduced due to the formation of a more stable complex $PdBr_4^{2-}$, as can be inferred by comparing the electrode potential (vs Normal Hydrogen Electrode, NHE) of Equations 3-5below.[16] We believe that this ligand replacement could significantly reduce the reduction rate in a similar way as Pd nanobars formation.[10a]However, unlike the synthesis of pure-Pd nanobar, the PdAg nanobar yield was not substantially changed by the manipulation in the Br^{-} ions concentration in the composition range studied here (Fig. 3).

$$Pd^{2+} + 2e^- \rightarrow Pd \qquad E° = 0.915 \text{ V vs NHE} \qquad (3)$$

$$PdCl_4^{2-} + 2e^- \rightarrow Pd + 4Cl^- \qquad E° = 0.59 \text{ V vs NHE} \qquad (4)$$

$$PdBr_4^{2-} + 2e^- \rightarrow Pd + 4Br^- \quad E° = 0.49 \text{ V vs NHE} \qquad (5)$$

3.3.2 Effect of the temperature. It is believed from thermodynamics that Pd atoms nucleate and grow into cuboctahedrons (with a nearlyspherical shape) enclosed by a mix of (111) and (100) facets to minimize the total surface energy. In general, an *fcc* metal can only be forced to grow into anisotropic nanostructures through the kinetic control. For instance, when the rate of atomic addition is sufficiently fast, the preferential growth on this particular face leads to the formation of an elongated nanostructure with a square cross-section. More specifically, when the reduction rate is in the medium region, the seeds take a cubic shape with slight truncation at the corners, and the product containsmainly nanobars. As the reduction rate becomes much faster, more seeds are formed in the nucleation step. These cubic seeds are smaller, but have more significant truncation at the corners, and the final product is dominated by nanorods thinner than the nanobars. [10a,17]In the present case, the Pd and Ag reduction was slower at lower temperature levels (Exp. 1, 3, 5 and 7) than at the higher ones since the product consisted mainly of irregular nanoparticles instead of PdAg nanobars (Fig. 1 and 2). This slow reduction was evident during the experimentation as the color change from reddish- brown to black, that indicates that the reduction of the precursors was slower, and that could have resulted from the addition of Ag^{+} ions to the reaction.The higher concentration of the more stable AgBr in the final product (see Fig.4 and Table 4) suggested another source of kinetics hindering; perhaps occasioned from to more negative reduction potential of Ag^{+} and AgBr, compared to the $PdBr_4^{2-}$ ions formed during the reduction process to obtain pure Pd nanobars by means of Equations 6 and 7.[10a,16a,16b]

$$Ag^+ + e^- \rightarrow Ag \qquad E° = 0.799 \text{ V} \qquad (6)$$

$$AgBr + e^- \rightarrow Ag + Br^- \qquad E° = 0.071 \text{ V} \qquad (7)$$
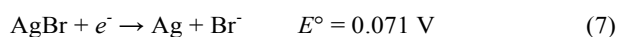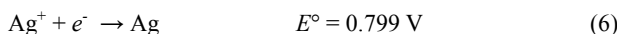
This kinetic obstruction of the reduction rate by silver species is supported by the strong suppression of the AgBr diffraction peaks observed at higher temperature levels, where the reduction rate increased leading to both: higher PdAg nanobar yields and lower AgBr production (See Table 4). In addition, the incorporation of

some silver atoms into the nanobar structure was evident by the lattice expansion observed when comparing the lattice parameter of the PdAg materials the pure-Pd material. This lattice expansion was more significant at high temperature levels.
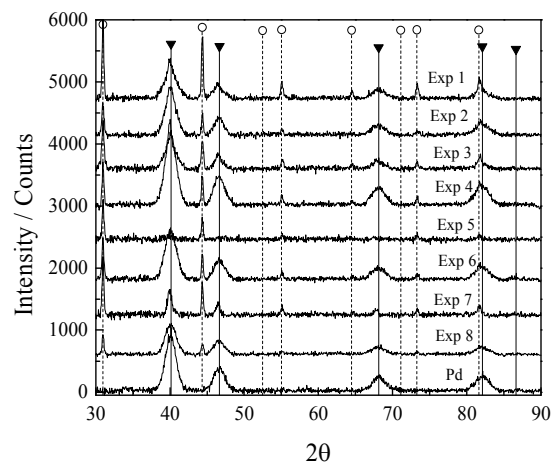

Fig. 4 XRD patterns of the eight experiments and pure Pd nanobars: (○) AgBr, (▼) Pd.

Table 4 Structural parameters and composition calculated by fitting the XRD patterns shown in Figure 4 using the Rietveld method.

Experiment	Pd Crystal size (nm)	Pd Lattice parameter (Å)	% AgBr
1	5.4	3.8976	25.9
2	5.8	3.8956	12.1
3	6.6	3.9012	24.6
4	5.6	3.8961	8.6
5	clusters	3.8760	100
6	5.4	3.8960	11
7	18.7	3.9094	54.12
8	5.8	3.8956	9.45
Pd	6.7	3.8847	0

3.3.3 Effect of the reaction time. In the case of pure Pd, it has been reported that the Pd nanobars can be formed via growth from small, near spherical seeds, or through the evolution of nanorods in an aging process.[10a]In the present study, the reaction time was found to be as important as the reaction temperature (see Table 3 and Fig. 3); the absence of nanorods in all the experiments points out towards PdAg nanobars formed from the small nanoparticles during the nucleation step. The similar width of the PdAg nanobars in all the experiments (5-7 nm, Fig. 1) also supports this argument because nanobars evolved from nanorods during the ageing process should have a thinner diameter.[10a] Lowering the concentration of AgBr in the low time level (Fig. 4 and Table 4) suggested that the Ag atom reduction took place through the more stable AgBr reduction pathway. On the other hand, the small yield obtained at 1 h reaction suggested that this time was not enough to allow the Pd and Ag atoms to incorporate to the nanoparticle. This significant dissimilarity between the Pd and PdAg nanobar formation time could be related to the differences of the

reduction potential already discussed in sections 3.3.1 and 3.3.2.

3.3.4 Interaction effects. Fig.5 illustrates the effect of interaction between three factors on the PdAg nanobar yield. Here it is possible to observe which interactions between factors are stronger for the nanobar yield formation. When the difference in the slope of the two lines at each cell is too large, the interaction between the two factors of the cell is strong.[11] At low reaction temperature level (-1), the nanobar yield remained almost unchanged, independently of the level observed in time and Br$^-$ concentration. On the contrary, at high temperature levels, the temperature-reaction time showed the strongest interaction effect, as the slope is markedly steeper than the temperature-Br concentration interaction.

If we look at the high levels (reaction time and temperature) in the KBr column we observed that the nanobar yield increased as the Br$^-$ concentration increased from low to high level. On the contrary, a diminution of nanobar yield was observed at low levels (temperature and reaction time) as the Br$^-$ concentration changed from low to high level. The individual and interaction effects already discussed can also be observed in Table 3, where the F values for the temperature, reaction time and temperature-reaction time interaction are the highest ones, thus showing the significance of these factors on the PdAg nanobar yield.
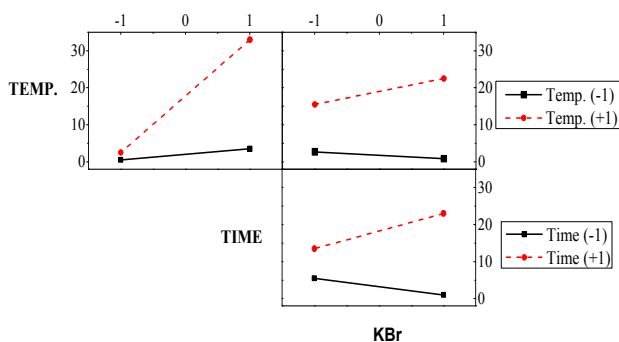

Fig. 5 Interaction effects plot (*y*-axes are the Main adjusted values for PdAg nanobar yield)

3.4 Optimization trials

According to the results from the previous sections, the temperature and reaction time must be controlled carefully due to their strong effect on the final product. Thus, three experiments were planned and executed in order to improve the PdAg nanobar yield. The analysis of main factors and interactions suggested that increasing the value of these factors would increase the nanobar yield.

Figure 6 shows the TEM results of the samples made under experimental conditions around Exp.8 (Table 2), which represented the highest yield from the full factorial design application. In the optimization trials, the Br$^-$ concentration remained unchanged at high level. The Figure 6a is the result obtained by increasing the temperature 13 K (413 K) while the reaction time remained at 3 h. In this case, the PdAg nanobar yield increased to 47.3 %. On the other hand, by increasing the reaction time to 4.5 h remaining the reaction temperature at 400 K resulted in a decreasing of the nanobar yied from 43 to 37.5 % (Figure 6b). Moreover, by increasing both temperature and reaction time (413 K, 4.5 h) resulted in a diminution of the

nanobar yield to 35.8 % (Figure 6c). This decreasing on the nanobar yield in Figure 6b and 6c could be due to the evolution from nanobars to irregular nanoparticles during the growth and/or aging process, as has been reported to occur for Pd nanobars.[10a] However, the 47.3 % of nanobar yield corresponds to the maximum value obtained under the experimental conditions analyzed, considering the impossibility to increase the temperature reaction due to the boiling point of the ethylenglycol-water mixture (413 K). The highest value of PdAg nanobar yield is comparable to other syntheses of Pd nanostructures with controlled morphology by chemical methods reported in the literature.[15,17]
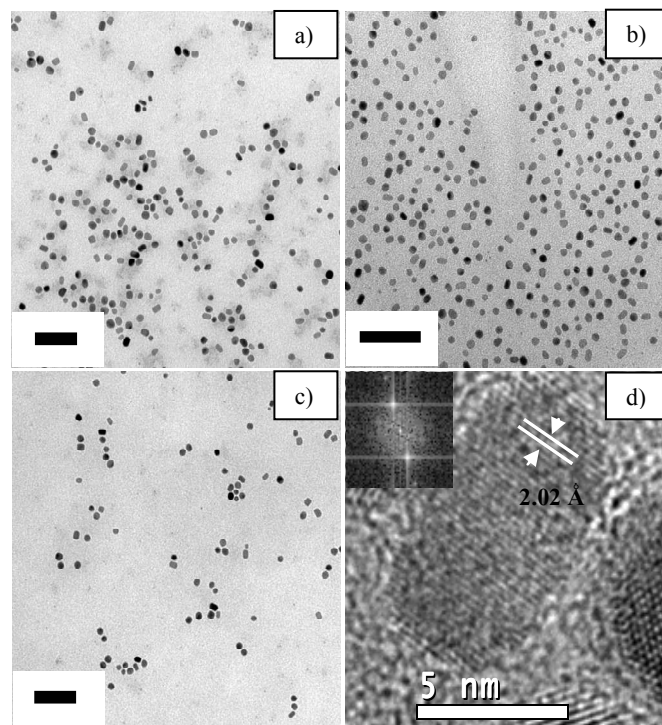

Fig. 6 TEM images for the experiments at: (a) 413 K, 3h, (b) 400 K, 4.5 h, (c) 413 K, 4.5 h, (d) HRTEM of a PdAg nanobar from (a), the inset is a FFT calculated from a beam perpendicular to the surface. Scale bar: 50 nm.

Fig.6d shows the HRTEM of a PdAg nanobar from Figure 6a. It is worth noticing that nanobar size was very similar in all the synthesis, as can be appreciated in Table 4 as well. It has been reported that when AgNO$_3$ is added at a moderate rate (during a seed-mediated process) into the Pd nanobar suspension, the Ag grows preferably on three adjacent faces of a Pd seed resulting in an eccentric heterostructure of PdAg and the formation of a Ag plate, cube, and then bar with slight truncations at the corners.[18] This phenomenon could explain the truncation of the PdAg nanobar observed in the present study, considering that the one-pot co-reduction process is similar to seed-mediated growth in nature because one metal ion will be reduced first due to the difference in the reduction potentials of the two metal cations. The pre-formed metal will serve as in situ seeds for the successive reduction and growth of another metal.[19] However, the surface of the PdAg nanobar seems very homogeneous and the interplanar distance calculated (Fast Fourier Transform) is closer to the Ag(200) instead of the Pd(200) (2.045 and 1.945 Å, respectively), perhaps due to the preferential growth of Ag discussed above that resulted in a Ag layer thin enough to avoid being observed by XRD. Moreover,

the HRTEM data indicated that the (200) faces observed in pure Pd nanobars are also observed in PdAg nanobars. This result is interesting because the preferential orientation of the PdAg nanobars could have catalytic effects on structure-sensitivity reactions, such as EOR

The surface composition for the nanoparticles shown in Fig.6a was analysed by XPS technique. The survey scan (Fig.7a) showed the presence of carbon and bromide residuals from the synthesis step. The atomic concentration at the surface was found to be 11.8, 28.3, 56.54, 1.94 and 1.4 for Pd, C, O, Br and Ag respectively. The high content of oxygen suggests the presence of a thin film of Ag and Pd oxides that commonly coexist at the surface of palladium nanoparticles exposed to the air,[19] which could not be detected by XRD patterns. Furthermore, the Pd/Ag atomic ratio calculated was 8.42, which corresponds to 89.5 and 10.5% of Pd and Ag, respectively (without considering impurities). This result is consistent with the composition obtained by EDX (section 3.1). Density Functional Theory studies already showed that clean Pd(100) displays a surface core level shift to lower binding energies in Pd 3d photoemission spectra, whereas a shift to higher binding energies relative to the bulk contribution is observed for $Pd_{75}Ag_{25}(100)$. This contribution is caused from Pd atoms embedded in the surface region of a silver terminated $Pd_{75}Ag_{25}(100)$ surface.[5a] The results obtained in the present work agreed with DFT results, as a small shift towards higher binding energy was found in Pd $3d_{5/2}$ (335.2 eV) and Pd $3d_{3/2}$ (340.4 eV) in comparison to Pd pure materials (dotted lines shown in Fig.7b).
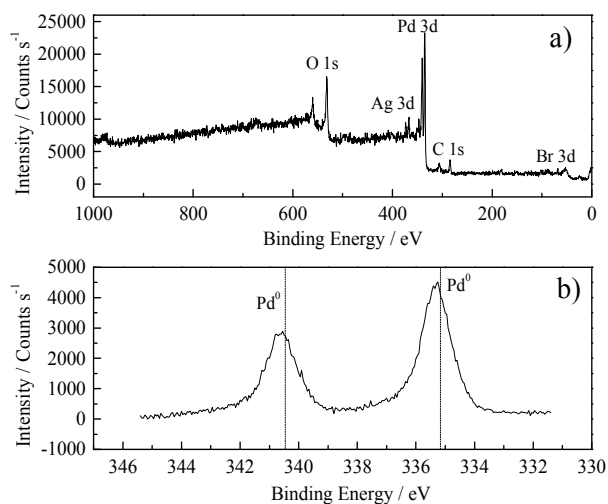

Fig. 7 XPS spectrum for the nanoparticles shown in Figure 6a.

3.5 Application of PdAg as catalyst

PdAg nanobars observed in Figure 6a and pure-Pd nanobars obtained by a methodology already reported[4b] were supported on carbon Vulcan to obtain a catalyst. These catalysts were tested for the ethanol electro-oxidation in 1 M KOH solution by cyclic voltammetry (Fig.8).The voltammograms were characterized by two well-defined current peaks: one in the anodic scan and the other in the cathodic scan. In the anodic scan, the oxidation peak was related to the oxidation of freshly chemisorbed species derived from ethanol adsorption. The oxidation peak in the reverse scan is associated with the removal of carbonaceous species that are not completely oxidized in the positive scan, rather than the oxidation of freshly chemisorbed species.[20]For the PdAg/C and Pd/C

catalysts, the onset potential of the EOR were -0.6 and -0.5 V, whereas the peak current densities were found at -0.13 and -0.12 V vs NHE respectively. Moreover, the peak current density for the bimetallic catalysts was 2.5 times higher than the pure-Pd catalysts. Since the PdAg and Pd nanobar size (length) was comparable (6.7 and 8 nm, respectively) for the electrocatalysts; the difference in the EOR activity should be associated to the different structure and elemental compositions on surface. The higher suppression of the hydrogen adsorption/desorption peaks (at E < -0.7 V vs NHE) in the Ag-containing catalyst was another evidence of surface modification, as it has been associated to the Pd surface alteration due to the introduction of Ag.[8c] The more negative onset, higher and more negative current peak potential showed that the incorporation of Ag in Pd nanobar improves the kinetic and thermodynamic behavior towards the EOR in comparison to that obtained on nanometric pure Pd nanobars. These pure Pd nanostructures have been identified as excellent electrocatalysts due their preferential exposition of Pd(100) faces which favor the adsorption and oxidationprocess of ethanol.[4b]
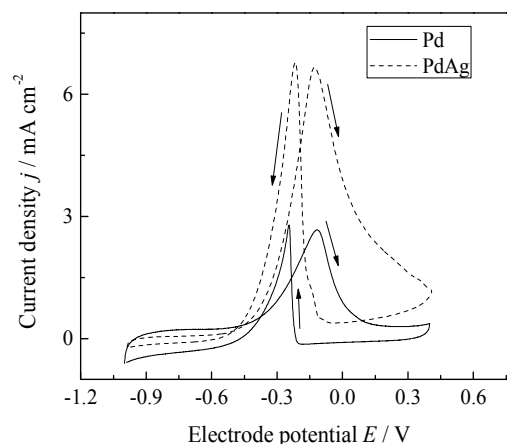

Fig. 8 Cyclic voltammograms obtained at 1M ethanol for the nanoparticles shown in Figure 6a and a squared-Pd/C catalyst. Experimental conditions: 1 M KOH, 40 mV s-1, electrode diameter = 3 mm, room temperature.

4 Conclusions

Factorial design methodology was applied to the synthesis and optimization of palladium/silver nanobars using the polyol process as reducer. The concentration of Br$^-$ ions, the temperature and time of the reaction were selected as factors to study, whereas the yield (% nanobars) and particle size were the expected responses to be analyzed. The nanoparticles were characterized by XRD, TEM, HRTEM and XPS. The three factors have a positive effect on the response, the nanobar yield increases as the level changed from -1 to +1. The temperature and reaction time presented the strongest effect on the nanobar yield; whereas the Br$^-$ concentration impacted to a less extent the nanobar formation. Temperature-reaction time had the strongest interaction effect on the PdAg nanobar yield.The 47.3 % of nanobar yield corresponds to the maximum value obtained under the experimental conditions analyzed, and showed for the first time, the possibility to reduce the Pd and Ag to generate PdAg bimetallic nanobars smaller than 10 nm (width). These bimetallic nanobars showed better electrocatalytic performance as the onset potential was 0.1 V more negative and the current density was 2.5 higher than pure Pd nanobars, which have been

reported to present excellent performance towards the EOR due to their preferential exposition of Pd(100) faces. This result exemplified the important catalytic properties that these nanobars could have, especially in the catalytic field where small size is often preferred.

Acknowledgements

Notes and references

1   E. Antolini and J. Perez, *J. Mater Sci.*,2011, **46**, 4435.

2   a) H. Erikson, A. Sarapuu, N. Alexeyeva, K. Tammeveski, J. Solla Gullon and J.M. Feliu, *Electrochim. Acta,*2012, **59**, 329; b) H. Erikson, A. Sarapuu, N. Alexeyeva, K. Tammeveski, J. Solla Gullon and J.M. Feliu, *Electrochem.Commun.*,2011, **13**, 734.

3   C. L. Lee and H. P. Chiou, *Appl. Catal. B: Environmental*,2012, **117-118**, 204.

4   a) E. D.Wang, J. B. Xu andT. S. Zhao, *J. Phys. Chem. C.*, 2010, **114**, 10489; b) R. Carrera Cerritos, M. Guerra-Balcázar, R. Fuentes Ramírez, J. Ledesma-García and L. G. Arriaga, *Materials*,2012, **5**, 1686.

5   a)L. E.Walle, H. Grönbeck, V.R. Fernandes, S. Blomberg, M.H. Farstad, K. Schulte, J. Gustalfson, J. N. Anderson, E. Lundgren and A. Borg, *Surface Science*,2012, **606**,23-24, 1777; b) I.H. Svenum, J.A. Herron, M. Mavrikakis and H. J. Venvik, *Catal., Today*, 2012, **10**, 193.

6   J.B. Xu, T.S. Zhao, Y. S. Li and W.W. Yang, *Int. J. Hydrogen Energy*,2010, **35**, 9693.

7   a) V. Bambagioni, C. Bianchini, A. Marchionni, J. Filippi, F. Vizza, J. Teddy, P. Serp and M. Zhiani,*J. Power Sources*,2009, **190**, 241; b) T. Maiyalagan and K. Scott, *J. Power Sources*,2010, **195**, 5246; c) W. Li and P. Haldar, *Electrochem. Commun.*,2009, **11**, 1195; d) R. Wang, S. Liao and S. Ji, *J. Power Sources*,2008, **180**, 205.

8   a) Q. Wang, J. Zheng and H. Zhang, *J. Electroanal.Chem.,*2012, **674**, 1; b) A. Godínez-García, J.F. Pérez-Robles, H. V. Martínez-Tejada and O. Solorza-Feria, *Mater.Chem. Phys.*,2012, **134**, 1013; c) G. Li, L. Jiang, Q. Jiang, S. Wang and G. Sun, *Electrochim. Acta*,2011, **56**, 7703.

9   a) S. T. Nguyen, H. M. Law, H. T. Nguyen, N. Kristian, S. Wang, S. H. Chan and X. Wang, *Appl. Catal. B: Environmental*,2009, **91**,507; b) E. H. Yu, U. Krewer and K. Scott, *Energies*, 2010, **3**, 1499.

10 a) Y. Xiong, H. Cai, B. J. Wiley, J. Wang, M. J. Kim and Y. Xia, *J. Am. Chem. Soc.,* 2007, **129**, 3665; b) M. Jin, H. Liu, H. Zhang, Z. Xie, J. Liu and Y. Xia, *Nano Res.*, 2011, **4,1**, 83.

11 J. H. Lim and J.S. Lee, *Colloids and Surfaces A: Physicochem. Eng. Aspects*, 2008, **322** 155.

12 S. J. Nejad, H. Abolghasemi, M. A. Moosavian, A. Golzary and M.G. Maragheh, *J. Supercritical Fluids*,2010, **52**, 292.

13 C. Vitorino, F. A. Carvalho, A. J. Almeida, J. J. Sousa and A. A.C.C Pais, *Colloids and Surfaces. B: Biointerfaces*,2011, **84**, 117.

14 M. M. Ba-Abbad, A. A H. Kadhum, A. B. Mohmad, M. S. Takriff and K. Sopian, *J. Ind. Eng. Chem.*,2013, **19**, 99.

15 W. U Binghui, Z. Huihui and Z. Nanfeng.[OL].[2012-02-15 14:02:47].http://www.paper.edu.cn/index.php/default/en_releasepaper /downPaper/201202-431(accessed October 2013).

16 a) A. J. Bard, R. Parsons, and J. Jordan in*Standard Potentials in Aqueous Solution (prepared under the auspices of the International Union of Pure and Applied Chemistry)*, Dekker, New York, 1985, G; b) G. C. Zoski in *Handbook of Electrochemistry*, Elsevier B.V., UK, 1st Ed., 2007, pp.815; c) Y. Xiong, J. M. McLellan, J. Chen, Y. Yin, Z. Y. Li and Y. Xia, *J. Am. Chem. Soc.* 2005, **127**, 17118.

17 Y. Xiong, H. Cai, Y. Yin and Y. Xia, *Chem. Phys. Letters*,2007, **440**, 273.

18 a) X. Liu, D. Wang and Y. Li, *Nano Today*, 2012, **7**, 448; b) J. Zeng, C. Zhu, J. Tao, M. Jin, H. Zhang, Z. Y. Li, Y. Zhu and Y. Xia, *Angew Chem. Int. Ed.*,2012, **51**, 2354.

19 C. M. Ghimbeu, C. Zlotea, R. Gadiou, F. Cuevas, E. Leroy, M. Latroche and C. Vix-Guterl, *J. Mater. Chem.*, 2011,**21**, 17765.

20 R.N.Singh, A. Singh and A. Anindita,*Carbon*, 2009, **47**, 271.

Full Factorial design methodology was applied for the first time to the synthesis and optimization of palladium/silver nanobars using the polyol process as reducer.